Nucleation of Pb starfish clusters on the five-fold Al-Pd-Mn quasicrystal surface

J. Ledieu[*]

Institut Jean Lamour, UMR 7198 CNRS - Nancy Université - UPVM, Ecole des Mines, Parc de Saurupt, 54042 Nancy Cedex, France

M. Krajčí

Institute of Physics, Slovak Academy of Sciences, Dúbravská cesta 9, SK-84511 Bratislava, Slovak Republic
and Fakultät für Physik and Center for Computational Materials Science, Universität Wien, Sensengasse 8/12, A-1090 Wien, Austria

J. Hafner

Fakultät für Physik and Center for Computational Materials Science, Universität Wien, Sensengasse 8/12, A-1090 Wien, Austria

L. Leung,[†] L. H. Wearing, and R. McGrath

Department of Physics and Surface Science Research Centre, The University of Liverpool, Liverpool L69 3BX, United Kingdom

T. A. Lograsso and D. Wu

Ames Laboratory, Iowa State University, Ames, Iowa 50011, USA

V. Fournée

Institut Jean Lamour, UMR 7198 CNRS - Nancy Université - UPVM, Ecole des Mines, Parc de Saurupt, 54042 Nancy Cedex, France

The nucleation of Pb clusters on the five-fold Al-Pd-Mn quasicrystal surface has been investigated using scanning tunneling microscopy (STM) and *ab initio* calculations based on density-functional theory (DFT). In the submonolayer regime, Pb atoms are highly mobile and adsorb preferentially within equatorially truncated pseudo-Mackay clusters present at the surface. The decoration of these unique adsorption sites leads to the formation of five-fold islands dubbed "starfish" and eventually to a quasiperiodic Pb monolayer. From a comparison of measured and calculated STM images it is concluded that most starfish clusters on all terraces are composed of ten Pb adatoms. A model of the structure of the starfish cluster has been proposed. Our total-energy calculations confirm its stability. The experimentally measured height profile of the starfish cluster is also reproduced by the DFT calculations.

I. INTRODUCTION

As their atomic structure is now relatively well understood,[1,2] quasicrystal surfaces are being used as templates for growth studies.[3–5] The choice of such complex intermetallic alloys as substrates is motivated by their aperiodic surface structure which exhibits long-range order but lacks translational symmetry. They also represent a fascinating testing ground to answer fundamental questions, as demonstrated recently[6] in a study of the role of aperiodicity on the electronic properties of a monoelement quasiperiodic thin film. Other phenomena such as quantum size effects (QSEs) influencing metallic thin-film growth on quasicrystal surfaces have triggered interest well beyond the quasicrystal community.[4] In addition, quasicrystal surfaces possess a relatively large variety of potential adsorption sites compared to "classical" crystal surfaces, offering the possibility of growing unusual surface structures with novel physical properties.[7,8]

Scanning tunneling microscopy (STM) studies with atomic resolution have identified two characteristic motifs on the five-fold Al-Pd-Mn surface. The pentagonal "dark stars"[9,10] and the "white flowers"[11,12] have been tentatively assigned to truncated pseudo-Mackay clusters. Together with Bergman clusters, these can be considered as the building blocks of the bulk icosahedral structure. This assignment has been confirmed by detailed simulations of the STM contrast based on *ab initio* density-functional calculations.[13] These simulations also showed that the dark star is the signature of surface vacancies originating from the irregular atomic arrangement around the low-coordinated Mn atoms in the center of the pseudo-Mackay clusters. As shown in previous studies,[7,8,14–16] these surface vacancies act as trap sites binding adatoms very strongly.

Cai *et al.*[14] reported the formation of pentagonal islands resembling "starfish" while dosing Al atoms on the five-fold Al-Cu-Fe surface, which is isostructural to the five-fold surface of icosahedral Al-Pd-Mn. It was proposed that pentagonal Al starfish clusters are formed by diffusion of an adatom to the dark star site, followed by the addition of five more Al atoms around its periphery. At increasing coverage, island growth is observed, which excludes the formation of a dense quasiperiodic overlayer. For Bi adsorption, STM measurements at submonolayer coverage reveal the formation of pentagonal islands on the five-fold Al-Pd-Mn surface. A quasiperiodic thin film is obtained upon completion of the first Bi monolayer. The initial nucleation sites have been recently identified as the centers of the white flower motifs.[16] These sites are theoretically populated by Mn atoms and have also recently been recognized as good candidates for Si adsorption.[15] The formation of starfish clusters at low coverage and the growth of a quasiperiodic single-element mono-

layer are also observed while dosing Pb on the five-fold Al-Pd-Mn surface.[6] However, in that work the preferential nucleation site leading to the starfish formation was undetermined.

A dual approach combining experimental results and *ab initio* DFT has been chosen. DFT calculations have been used previously[2,7,8,17–19] to calculate the geometric and electronic structures of the surfaces of quasicrystalline approximants and of pseudomorphic adlayers formed on these surfaces. Using the results for the surface electronic structure, simulated STM images[13] were generated and the good agreement with experimental images confirmed the validity of the theoretical structure models.

Ab initio density-functional calculations have also been used to explore stable and preferential adsorption sites, to understand the required conditions for the formation of a quasiperiodic single-element monolayer (optimum atomic size, film density) and to probe the surface reactivity of the five-fold Al-Pd-Mn surface.[7,8,19] The calculations have demonstrated that unsupported quasiperiodic monolayers are not stable and that quasiperiodic ordering in an adsorbed monolayer results from the strong binding of adatoms to quasiperiodically distributed adsorption sites.[7]

A Penrose P1 tiling consisting of pentagons, pentagonal stars, boats, and thin golden rhombi can be superimposed on the atomic structure of the five-fold surface.[11] The vertices of the P1 tiling coincide with the positions of Pd atoms located in the center of the Bergman clusters. For the group IV and V elements Bi, Sn, and Sb, the largest binding energies of single adatoms are found at surface vacancies, vertices and midedge position of the P1 tiling, and on Mn surface atoms.[7]

For adatoms from groups I to III of the Periodic Table, it has been shown that they occupy surface vacancies, vertices of the P1 tiling, and quasiperiodically distributed charge-density minima.[18,19] Surface vacancies bind adatoms most strongly, but atoms trapped in these sites are incorporated in the surface layer and do not form part of the quasiperiodic adlayers. It is found that in addition to strong binding at quasiperiodically distributed sites, the atomic radius of adatoms and the overlayer density play a crucial role in determining the stability of the quasiperiodic ordering of the absorbed monolayer.[19]

Relaxation of a complete Na or K monolayer with an initial structure conformal with the P1 tiling is predicted to lead to a spontaneous rearrangement of the atoms and the formation of a highly ordered pseudomorphic overlayer which can be described using a DHBS tiling composed of decagons (D), squashed hexagons (H), boat-shaped tiles (B), and pentagonal stars (S).[18] The P1 and DHBS tilings are both equivalent descriptions of the five-fold surface of icosahedral Al-Pd-Mn, but for the adsorbed alkali monolayers, a structure based on the DHBS tiling allows a more regular distribution of the atoms decorating the interior of the tiles. Interestingly, the decagonal rings of adatoms in the DHBS tiling coincide with the white flower motifs.

The aim of the investigations presented here is to identify the nucleation sites leading to the formation of Pb "starfish" clusters on the five-fold surface of icosahedral Al-Pd-Mn and the elucidation of their precise atomic structure. Experimental investigations were carried out using low-energy electron diffraction (LEED) and high-resolution STM. They are complemented by *ab initio* DFT calculations which determine the most stable adsorption sites of isolated Pb atoms and the mechanism of formation of the starfish clusters. Finally, simulated STM images are compared to the experimental ones.

II. EXPERIMENTAL DETAILS

The $Al_{70}Pd_{21}Mn_9$ sample provided by the Ames Laboratory was grown using the Bridgman method. The quasicrystal was cut perpendicular to its five-fold axis.[20] Prior to insertion into ultrahigh vacuum, the five-fold surface was polished with graded diamond paste down to $1/4$ μm; this procedure is described in detail elsewhere.[11] The preparation of the sample consisted of cycles of Ar^+ sputtering (2 keV) and annealing to 910 K. The temperature was monitored using an optical pyrometer with the emissivity set to 0.35. The structure of the surface was investigated using LEED and STM. The STM measurements presented here were done at room temperature in a constant current mode using an Omicron variable-temperature STM. The surface was considered to be clean when no traces of contaminants (mainly oxygen and carbon) could be detected by x-ray photoelectron spectroscopy (XPS). Lead deposition was achieved using an electron-beam cell. The Mo crucible was loaded with lead wires (99.999%) and the flux was set to 2.5×10^{-3} ML/s. The Pb source was calibrated by means of XPS and STM using an Al(111) crystal. A coverage of one monolayer (ML) was determined using STM by measuring the fractional area covered with successive Pb depositions. STM images of Pb clusters were scanned at a voltage of +2.3 V and a constant tunneling current of 0.5 nA.

III. COMPUTATIONAL DETAILS

The theoretical investigations are based on DFT. We have used the Vienna *ab initio* simulation package (VASP) (Refs. 21 and 22) to perform *ab initio* electronic structure calculations and structural optimizations. VASP performs an iterative solution of the Kohn-Sham equations within a plane-wave basis. A semilocal gradient-corrected functional[23] (PW91) is used to describe electronic exchange and correlation. The projector-augmented wave (PAW) method[22,24] is used to describe the electron-ion interactions. PAW calculates the exact all-electron potentials and charge densities; hence it produces very realistic valence-electron distributions. The energy-resolved charge-density distributions are the essential input information for the calculation of simulated STM images. STM images of surfaces and adsorbates have been calculated according to the Tersoff-Hamann approximation.[25] STM images actually reflect the electronic charge density at a certain distance above the surface and energies slightly above or below the Fermi level (depending on the position of the tip, the tunneling voltage and the direction of the current). The positive scanning voltage of +2.3 V used at the calculation corresponds to contributions from unoccupied states up to 2.3 eV above the Fermi level.
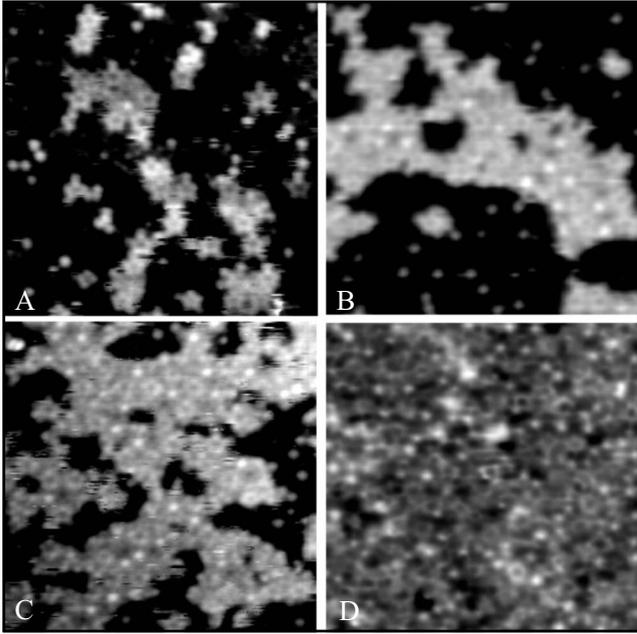
FIG. 1. (a) 180 Å×180 Å STM images of the five-fold Al-Pd-Mn dosed with (a) 0.20 ML, (b) 0.50 ML, (c) 0.76 ML, and (d) 1 ML of Pb, respectively.

As in our previous studies[7,8,17,18] a model for the structure of the five-fold surface of i-Al-Pd-Mn is derived from periodic approximants to the Katz-Gratias-Boudard (KGB) model[26–30] of the icosahedral structure. A model for the surface was constructed by cutting a thick slab perpendicular to one of the five-fold axes from the bulk structure. Details are given below.

The structure and exact location of the adsorbed Pb clusters are not known *a priori*. The construction of possible model structures is based on the exploration of the potential-energy landscape of an isolated adatom adsorbed on the surface. Idealized models consist of Pb atoms placed in and around the energetically most favorable adsorption sites. The stability of the Pb clusters formed on the i-Al-Pd-Mn surface is probed by performing a conjugate-gradient relaxation of the structure of the cluster/substrate complex under the action of the Hellmann-Feynman forces derived from the *ab initio* DFT calculations. The calculated total energies allow evaluation of the relative stability of the clusters.

IV. EXPERIMENTAL RESULTS

A. Characterization of Pb growth mode

We first characterize the Pb growth mode on the five-fold Al-Pd-Mn surface up to one ML. As shown on Fig. 1(a), the formation of pentagonal clusters (starfish) is already visible at 0.20 ML. Their edge length of 4.9 ± 0.3 Å is measured between the pentagonal vertices of highest intensity. Their overall size is however much larger and this will be further discussed in Secs. V and VI. These clusters of identical dimensions and of monoatomic height point in the same direction across terraces[6] and are observed independently of the flux used, ranging here from 2.5×10^{-3} ML/s to 2.5

$\times 10^{-2}$ ML/s. When deposited on the surface, Pb adatoms diffuse until they reach a trap site, i.e., a minimum in the potential-energy surface. The horizontal streaks ("fuzziness") recorded in the STM images are indicative of the displacement of Pb atoms on the surface by the STM tip. Additional Pb atoms agglomerate around this trapped atom if the lateral interactions and the binding to the substrate are strong enough to stabilize a cluster. If these adsorption sites are closely spaced and arranged in pentagonal symmetry, a starfish will be created. The fixed orientation of the starfish obtained regardless of the deposition rate makes it reasonable to postulate that initially Pb atoms nucleate preferentially at a precise site and the nucleation can be referred as heterogeneous. A comparable adsorption phenomenon (although at a different nucleation site) has been described by Cai *et al.*[14] for Al deposition on the five-fold Al-Cu-Fe surface and their interpretation of the experimental observations was supported theoretically using kinetic Monte Carlo simulations.[31]

Upon further adsorption [see Fig. 1(b)], the number of Pb starfish increases and isolated adsorbates are also distinguishable. At 0.76 ML, the film structure can be described as a network formed by interconnected starfish clusters. Although several starfish have still to be completed, additional Pb adatoms landing on the already deposited film fill the interstices of this network. This leads eventually to the completion of a full ML of Pb [see Fig. 1(d)]. It was not possible to grow a second layer with the flux ranges used here. The reason for such a drastic reduction in the sticking coefficient is still not fully understood. The density of the film measured by XPS (Ref. 6) is comparable to one ML of Pb adsorbed on the Al(111) crystal surface. A sharp five-fold LEED pattern is recorded at all coverages. The quasiperiodicity of the distribution of the adsorbed Pb atoms is further confirmed by fast Fourier transform calculations carried out on the STM images with only adatoms selected using a thresholding image analysis tool.

B. Identification of Pb adsorption site

We now concentrate on the identification of the nucleation sites leading to the formation of the starfish clusters and hence the quasiperiodic Pb monolayer. Figures 2(a) and 2(b) show STM images of the same region recorded at time intervals of a few minutes. On both images the quasicrystalline surface is well resolved and three starfish clusters are clearly identified. White circles outline the main topographical differences between both images. The circles are either filled, partially filled (streaks), or empty. The tip-induced motion and a relatively high mobility of the Pb adatoms could explain the differences in the site decoration from one image to the next. However, several isolated Pb atoms experience a stronger interaction with the substrate and do not move while scanning. One such adatom is marked in both images by a black circle.

The comparison of radial distribution functions derived from autocorrelation functions with those from model structures, which requires STM images with well resolved adatoms, was successfully used to identify the preferential nucleation site of Si on the Al-Pd-Mn surface at low
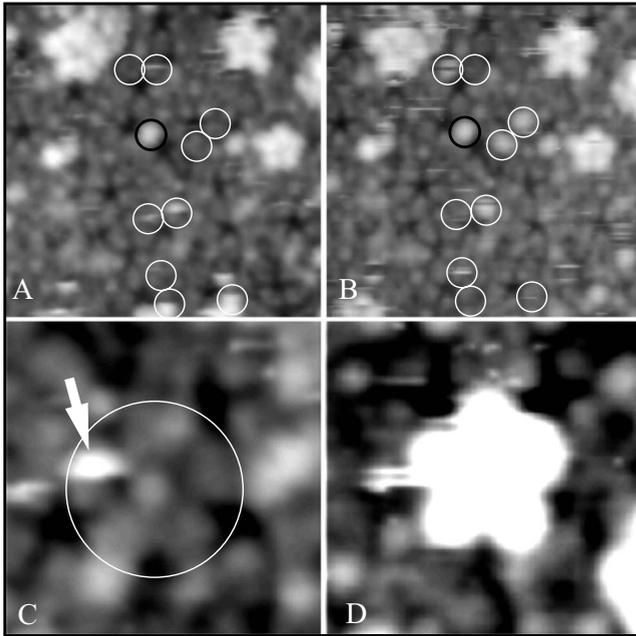
FIG. 2. [(a) and (b)] 97 Å×97 Å high-resolution STM images recorded minutes apart from the same region of the five-fold Al-Pd-Mn dosed with 0.15 ML of Pb. The white circles in (a) and (b) indicate the main differences in the Pb occupation. The circles outline also the preferential initial nucleation sites of the adsorbates. [(c) and (d)] 34 Å×34 Å STM images selected from (a) and (b) showing, respectively, a truncated Pseudo-Mackay cluster, surrounded by five truncated Bergman clusters from the substrate (also called the "white flower") and a pentagonal star formed by Pb adatoms. The arrow in (c) points to a Pb adatom partially scanned (half a circle) and the white circle encircled the white flower.

coverage.[15] As the formation of starfish clusters begins already at very low coverage, the number of isolated adatoms is very low. This growth mode considerably limits the usefulness of the above-mentioned image analysis procedure for the identification of preferential nucleation sites for single Pb atoms—if these exist at all. However, as will be shown later on, this approach can be used to determine the possible nucleation sites for the formation of a complete starfish.

An alternative to this approach is to investigate the local atomic arrangements around single Pb atoms and to measure the starfish-to-starfish distances on several terraces. In Fig. 2(c), one can recognize two features characteristic of the STM pictures. One consists of an equatorially truncated pseudo-Mackay cluster surrounded by five truncated Bergman clusters—i.e., the white flower discussed in Sec. I. The second is the dark star generated by a surface vacancy in the low-coordinated shell surrounding a Mn atom in the center of a pseudo-Mackay cluster located below the surface. The white arrow [Fig. 2(c)] points to a bright patch which corresponds to a half-scanned Pb adatom. This scanning effect allows us to estimate the adsorbate location. This Pb atom appears to sit on top of one of the five truncated Bergman clusters of the white flower. A careful analysis of several STM images shows that the same nucleation site is observed in all cases. In addition, all atoms outlined in Figs. 2(a) and 2(b) are positioned on top or in the close vicinity of a trun-

TABLE I. Theoretical and experimental maxima measured on radial distribution functions calculated from autocorrelation patterns derived from STM images obtained on a surface dosed with 0.2 ML of Pb. The experimentally measured starfish-to-starfish distances are compared to theoretical inter-"white flower"-to-"white flower" (WF-WF) distances.

WF-WF (Å)	Starfish-starfish (Å)
12.5	12.7 ± 0.5
20.3	21.5 ± 0.9
32.9	31.9 ± 1.3
38.6	35.6 ± 1.4
43.5	42.1 ± 1.7
52.2	51.0 ± 2.0

cated Bergman cluster. In contrast to previous studies,[10,15] the central Mn atom of the equatorially truncated pseudo-Mackay cluster as well as the dark stars are always visible, indicating that at this coverage no adatoms are adsorbed at these sites.

Figure 2(d) exhibits one isolated starfish already completed at 0.15 ML. For analysis purposes, the contrast of Fig. 2(d) has been saturated and the overall dimension of the starfish appears to be considerably larger compared to the value previously reported.[6] This pentagonal island is surrounded by five dark stars and is oriented parallel to the pentagon of the white flower in Fig. 2(c). From the positions of the five dark stars forming pentagons with edge length 12.8 ± 0.6 Å (the theoretical value[11] being 12.55 Å) and their orientation, we can conclude, after comparison with the theoretical model (see Sec. V), that the starfish cluster is formed on top of a white flower.

To confirm the white flower as the preferred site for Pb nucleation, the distances between the starfish clusters have been extracted from radial distribution functions obtained from autocorrelation patterns. To perform these calculations, the centers of the pentagonal islands are taken as reference points. They should correspond to the centers of the equatorially truncated pseudo-Mackay clusters, i.e., to the center of white flowers. Table I lists the theoretical white flower to white flower distances and the experimental starfish-starfish distances measured on the STM images. The agreement between the values in both columns is very good and confirms that starfish clusters nucleate on top of the WF's.

In the following section, *ab initio* total-energy calculations are used to determine the optimal location and shape of a Pb cluster. Simulated STM images derived from the calculated electronic structure are compared with experimental results.

V. THEORETICAL MODELING BASED ON *AB INITIO* DFT CALCULATIONS

A. Clean surface model

As in our previous *ab initio* studies[7,13,17–19] a model of the surface has been derived from the KGB model[26–30] of bulk *i*-Al-Pd-Mn. The atomic structure of the five-fold surface is derived from the structure of an icosahedral approximant by
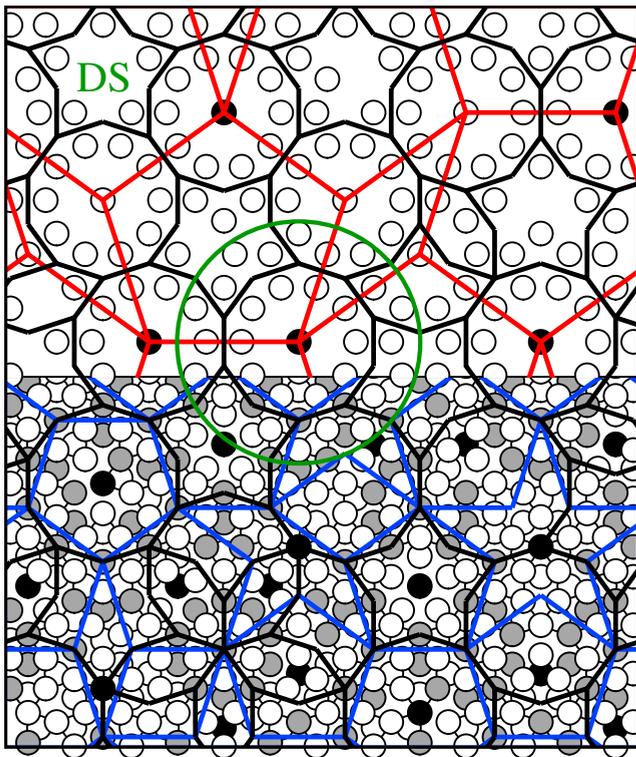
FIG. 3. (Color online) A model of the atomic structure of the five-fold surface of *i*-Al-Pd-Mn derived from a 5/3 approximant. The circles represent the atoms: Al—open circles, Pd—shaded circles, Mn—black circles. The quasiperiodic structure of the five-fold surface can be described by a DHBS tiling (black lines) or a P1 tiling (blue, gray lines). One complete white flower is marked by the green (gray) circle. One dark star is labeled explicitly as DS (green, gray). Lower half: All atoms seen at the surface are shown, together with the relation between the DHBS and the P1 tiling. Upper half: Only the positions of the atoms in the topmost atomic layer are shown, together with the relation between the DHBS tiling and the τ-scaled P1 tiling (red,gray).

cleaving at a plane perpendicular to one of the five-fold axes. The position of the cleavage plane was chosen such as to create a surface of high atomic density.[32] Planes with high atomic density are separated by gaps of low atomic density. The gaps in the atomic density between high-density planes are natural cleavage planes of the quasicrystal.[32] A detailed comparison between experimental surface data and structural models for the surface has recently been presented by Unal *et al.*[1] Their analysis confirms the present choice of a cleavage plane resulting in an Al-rich top layer and a high concentration of Pd in a layer only slightly below the surface.

The atomic structure of the *i*-Al-Pd-Mn quasicrystal can be interpreted in terms of interpenetrating pseudo-Mackay and Bergman clusters.[33] This cluster structure of the quasicrystal can also be recognized at the surface. Figure 3 shows a view of the atomic structure of the five-fold surface. The model has been constructed from the 5/3-approximant to the bulk quasicrystal. The quasiperiodic arrangement of the atoms at the surface can be described by a planar tiling. The choice of this tiling is, however, not unique. One possible choice relating to the cluster structure of the bulk quasicrys-

tal is a P1 tiling[32] consisting of regular pentagons, pentagonal stars, boats, and thin golden rhombi. Most of the vertices of the P1 tiling coincide with the centers of the Bergman clusters. The centers of the pentagonal tiles correspond to the positions of the pseudo-Mackay clusters. Figure 3 shows also the atomic structure of the surface. The top plane is Al-rich and contains a few Mn atoms, but no Pd. A second atomic layer, which is located only 0.48 Å below the surface, is decorated in a proportion of about 50/50 by Al and Pd atoms plus a few Mn atoms. The quasiperiodic arrangement at the surface can also be described by a DHBS tiling. Most vertices of the DHBS tiling coincide with the positions of Pd atoms in layers lying 0.48 Å and 1.26 Å below the surface plane. The D tiles have a direct relation to the white flower features seen in the STM images of the clean surfaces. In the topmost layer the vertices of the D tiles coincide with the centers of small pentagons of Al atoms (with an edge length of 2.96 Å) forming "petals" of the white flowers. The centers of white flowers represented by the D tiles have been identified as the nucleation centers for the Pb starfish clusters.

The S tiles in Fig. 3 have two orientations. They are decorated by five Al atoms located in the star arms, plus 0 to 2 other Al atoms in the interior of the tile. The irregular decoration of the S tiles is a consequence of the low and irregular coordination of the Mn atoms in the center of the pseudo-Mackay clusters, located below or above the surface. The S tiles with empty interiors are seen in STM images of the clean surface as dark stars. In Fig. 3 one such S tile is explicitly marked. As dark stars have always the same orientation, they are helpful in determining the orientation of the whole surface. The determination of the orientation of the adsorbed starfish clusters with respect to the surface is an important clue in the elucidation of the atomic structure of the starfish.

In Fig. 3 (top half) a τ-scaled P1 tiling (τP1, τ is the golden mean 1.618…) and its relation to the DHBS tiling are shown: in general, the vertices of the τP1 tiling coincide with the centers of the D tiles. In Sec. IV B it was concluded on the basis of a comparison between the distances between white flowers and the distances between starfish clusters that the nucleation of starfish clusters takes place on top of the white flower pattern, i.e., on top of a decagon of the DHBS tiling. Therefore in the next step we explore the potential-energy surface for the adsorption of an isolated Pb atom on different possible adsorption sites within a D tile using *ab initio* DFT calculations. These results are then used to construct models for the atomic structure of a starfish cluster.

The adsorption studies have been performed on a slab model of the five-fold surface derived from the 2/1 approximant to the quasicrystalline structure, as shown in Fig. 4. The thickness of the slab is 13.2 Å and consists of 19 atomic planes. This large thickness was found to be important to achieve well-converged binding energies for the adsorbates. Positions of all atoms in the slab, except the atoms in the bottom atomic plane were relaxed together with the positions of the adsorbed atoms. The atoms in the bottom plane were kept at fixed ideal positions. Neighboring slabs are separated by a 10 Å thick vacuum layer. Periodic boundary conditions have been applied. The computational cell has an orthorhom-
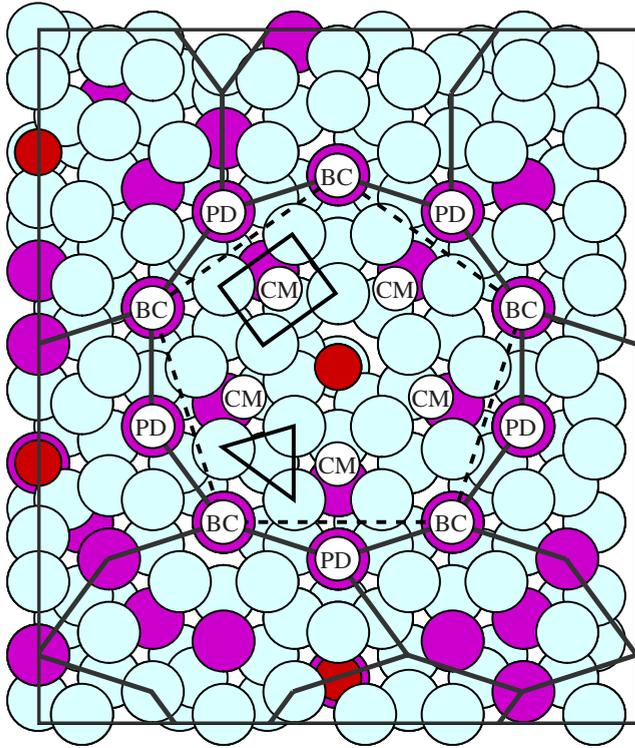
FIG. 4. (Color online) Possible adsorption sites on the five-fold surface of i-AlPdMn. The model of the five-fold surface is derived from a 2/1 approximant. The circles represent positions of the atoms: Al—pale (cyan) circles, Pd—dark (magenta) circles, Mn—small dark (red) circles. BC sites are centers of the Bergman clusters, PD sites are located above Pd atoms. Electronic charge-density minima in the surface are labeled CM. The BC sites form a pentagon of the P1 tiling (marked by dashed lines). The sites marked by the rectangle (R) and the triangle (T) are used also to label the orientation of adsorbed pentagonal clusters with respect to the five-fold symmetry of the surface.

bic shape, and contains 472 atoms. The surface unit cell measures 20.31 Å × 23.88 Å.

B. Geometric structure and total energy of Pb clusters

The protrusions displaying the highest intensities in the STM image of a starfish cluster (Fig. 2) form a pentagon with an edge length of 4.9 ± 0.3 Å. Hence our first guess of the atomic structure of a starfish cluster was that it is formed by five Pb atoms located at the vertices of a pentagon with an edge length of ≈5 Å. It was also expected that the Pb atoms are located in hollow sites (charge-density minima) of the surface. In our previous DFT study[19] we found that the hollow sites at the surface are stable adsorption sites for all elements from groups I to III. However on the *i*-Al-Pd-Mn surface there are no such stable adsorption sites with a local pentagonal symmetry and a lateral distance of ≈5 Å.

In Fig. 4 we have marked several possible adsorption sites in the D tile which exist in pentagonal patterns. The BC sites coincide with the center of Bergman clusters. These are hollow sites surrounded by five Al atoms and located above a Pd atom 1.26 Å below the surface plane. The BC sites form a
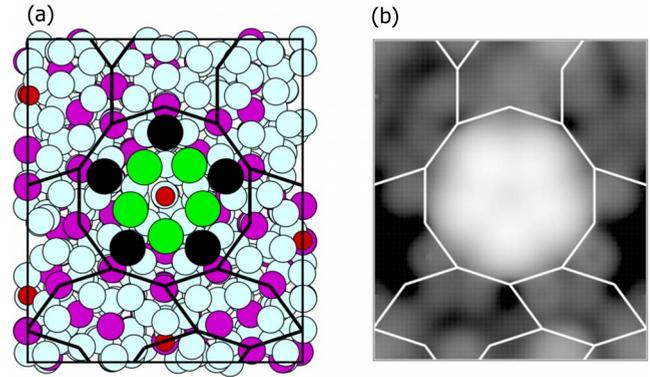

FIG. 5. (Color online) (a) Pentagonal Pb_5 clusters on the five-fold surface of i-AlPdMn. The black circles represent the positions of Pb adatoms in the $D5T_0$ cluster. The large green (pale) circles show the positions of Pb adatoms in the D5R cluster. Other circles represent atoms of the surface, cf. Fig. 4. (b) The calculated STM image of the D5R cluster.

pentagons of the P1 tiling (shown by the dashed lines in Fig. 4) with an edge length of 7.78 Å. The PD sites coincide with the positions of Pd atoms 0.48 Å below the surface plane. They can also be considered as hollow sites. As BC and PD sites occupy alternating vertices of the decagons of the DHBS tiling, they also form a pentagon with the same edge length of 7.78 Å, rotated by 36° with respect to the pentagon of BC sites.

In the electronic charge-density distribution of the clean surface one can recognize[19] a set of charge-density minima (CM) around the center of the D tile. The CM sites are located in the center of a rectangle R formed by four Al atoms (see Fig. 4). However, while the outer two Al atoms are in surface plane, the inner two Al atoms are in the next plane 0.48 Å below the surface plane. The CM sites form a pentagon with an edge length of ≈3.6 Å, concentric with the D tiles. Another important site discussed below is the triangle T.

We have made several attempts to find the correct atomic structure of the starfish cluster. In the first attempt we simply put five Pb atoms around the center of the D tile forming a pentagon with an edge of 5 Å. This choice was motivated by the size and the orientation of the starfish as seen in Fig. 2(d). The initial atomic positions in this cluster were in bridge sites between two Al atoms belonging to the triangle in Fig. 4, shown as the black circles in Fig. 5(a). This cluster is labeled as $D5T_0$ (the labeling of the clusters has been introduced to simplify the discussions). The $D5T_0$ cluster proved to be unstable. The structural relaxation under the Hellman-Feynman forces demonstrated that the Pb adatoms moved inwards or outwards, depending on their precise location with respect to the Al-Al bridge site which was found to be a saddle point of the potential-energy surface. When the adatoms moved outwards they finished in the BC sites.

The second model for the structure of the starfish labeled D5R is shown in Fig. 5(a) by the large pale (green) circles. The five Pb atoms occupy CM sites around the center of the D tile. The D5R cluster is stable with a high binding energy of −4.012 eV/Pb atom (see Table II). However, the D5R

TABLE II. Binding energies E_b of Pb atoms in the (meta)stable clusters. The labeling of the clusters is explained in the text.

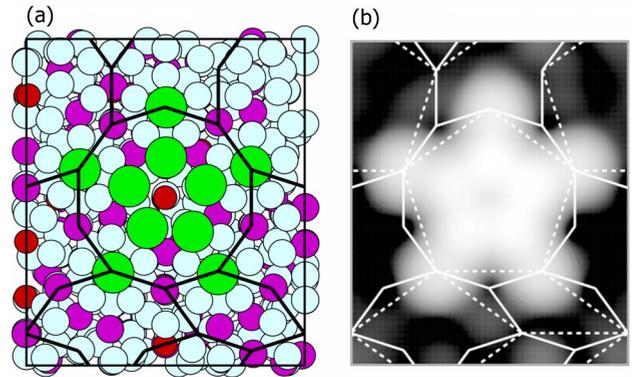| Cluster	Composition	E_b (eV/Pb atom)
D5R	5 CM sites	−4.012
D5B	5 BC sites	−3.951
D10R	D5R+D5B	−3.960
D10T	D5T+D5B	−4.057

FIG. 6. (Color online) (a) The large pale (green) circles show the positions of Pb adatoms in the D10T cluster in the BC sites and on top of the Al atoms surrounding the center of the D tile. The cluster has the correct orientation, it is stable, and has the lowest energy among all tested configurations. Other circles represent atoms of the surface, cf. Fig. 4. (b) The calculated STM image of the D10T cluster has the correct size and orientation. The P1 tiling is shown by the dashed lines.

cluster does not provide an STM image in agreement with the experimental image of the starfish. In experiment the starfish clusters are observed only with one specific orientation with respect to the five-fold symmetry of the underlying quasiperiodic surface. In the figures presented in this paper the correct orientation of the cluster is described by a pentagon pointing "up." This orientation is the same as that of the dark star (see Fig. 3). The pentagonal shape of the D5R cluster is pointing "down," although in the calculated STM [see Fig. 5(b)], its wrong orientation can be hardly recognized, as the characteristic pentagonal arms are missing.

The failure of our attempts to find a stable pentagonal Pb_5 cluster with the correct size and orientation therefore led us to test models where the starfish consist of two sets of adsorption sites with ten Pb atoms altogether. In our next attempt we tested whether the $D5T_0$ cluster could be stabilized by the presence of an inner shell isostructural to the D5R cluster. For this model the orientation of the outer pentagon is correct, and the distance between the outer Pb atoms corresponds to the measured size of the starfish. However, upon relaxation the structure proved to be unstable: the Pb atoms forming the outer pentagon moved outwards again and finished in the BC sites.

This led us to conclude that the BC sites must be part of the starfish cluster. The set of five Pb atoms occupying five BC sites around the D tile are labeled as D5B. The D5B cluster alone is too large to give the correct STM contrast of the starfish. However, we have found that the D5B cluster plus an inner shell formed by a modified $D5T_0$ cluster form a stable arrangement as shown in Fig. 6(a). The modified cluster denoted as D5T differs from $D5T_0$ by its smaller size. In their equilibrium positions the five inner Pb atoms form a pentagon of edge length 3.45 Å, and the distance between the inner and outer Pb atoms is 3.7 Å. Both distances are close to the nearest-neighbor distance in face-centered-cubic Pb. The D5T cluster alone is unstable, but if it is surrounded by a D5B ring, a stable structure results. The calculated binding energy of this cluster is −4.057 eV/Pb atom. This is the lowest energy configuration we have found (see Table II). This stable cluster of ten Pb atoms is labeled D10T.

Another (meta)stable structure with a correct orientation is a D10R cluster consisting of an outer ring of five Pb atoms in D5B positions and an inner cluster in D5R positions, i.e., the inner part of the cluster is rotated by 36° compared to the D10T structure. The binding energy of this configuration is −3.96 eV/Pb atom, i.e., altogether it is energetically less favorable by 0.97 eV/cluster. Moreover, the calculated STM image (not shown) is not satisfactory as it consists of a central D5R part surrounded by five separated spots corresponding to the D5B sites.

For the D10T the simulated STM contrast [Fig. 6(b)] matches well with the experimental images (see Figs. 6–8). The calculated STM contrast depends very sensitively on the exact lateral and vertical coordinates of the atoms. The inner Pb atoms occupying D5T sites are located at a distance of 2.93 Å from the center of the D tile and 2.27 Å above the surface plane. The outer D5B positions are 6.8 Å away from the center and only 2.05 Å above the surface.

This difference in the atomic heights of 0.22 Å corresponds well to the experimental estimate derived from the profile of the STM intensities. Figure 7(a) exhibits an experimental image of a complete Pb starfish where five protrusions of highest intensity (lightest color) form a pentagon of edge length equal to 4.9 ± 0.3 Å as described above. From the figure it is clear that the overall dimensions of the starfish cluster appear to be much larger: elongated "arms" reach out much further from the center. To understand the size of the starfish cluster, a one-dimensional profile along one of the starfish arms has been measured and plotted [see the red curve (gray) in Fig. 7(b)]. This profile shows a peak labeled by P and a shoulder S, with an estimated height difference of 0.35 Å. Profile measurements on several STM images lead to similar observations, with height differences ranging from 0.19 to 0.46 Å. We have calculated the STM profile of the starfish along the same path [see Fig. 7(b)]. Although there is certain discrepancy in the lateral extension of the curves caused presumably by dragging of the adatom by the STM tip during the measurement both curves exhibit the same characteristic features: the minimum at the center followed by a peak (P) and a shoulder (S). The lateral separation of the peak and the shoulder confirm that the pentagonal island contains ten Pb atoms in two distinct pentagonal sets.

In Fig. 8 we present a direct comparison of the calculated STM contrast of the D10T cluster with the experimental image of an isolated starfish—evidently agreement is very good. The STM image shows also a larger Pb island with clearly distinguishable pentagonal features with dark centers whose positions correspond to a pentagon of the τ-scaled P1
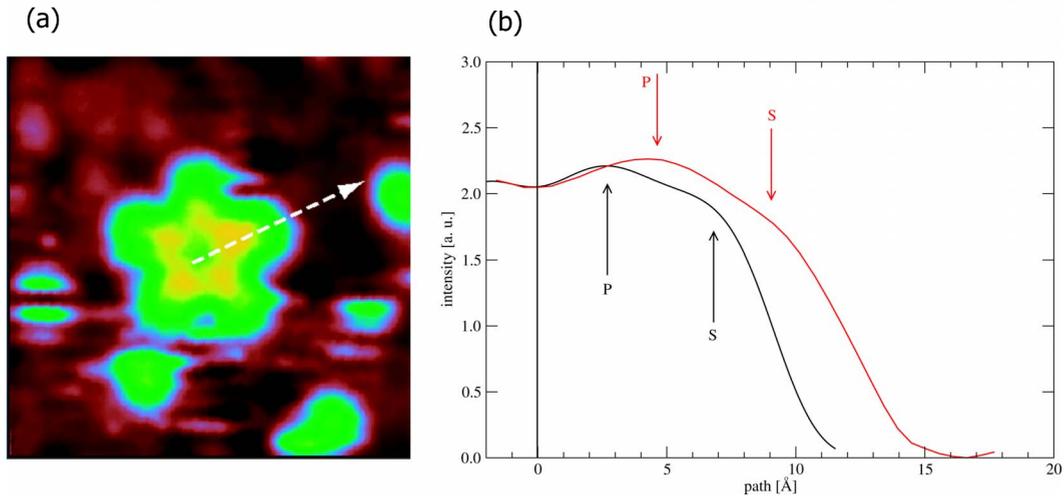
(a)

(b)

FIG. 7. (Color online) (a) 40 Å × 40 Å STM image showing a complete starfish. Although the overall cluster size is comparable to the one presented in Fig. 2(d), five brighter protrusions (highest intensity) form the pentagonal starfish of edge length equal to 4.9 ± 0.3 Å. (b) A comparison of the calculated (black) and measured (red, gray) one-dimensional profiles taken along the path represented by the arrow in (a). Both curves show a minimum at the origin, a peak labeled P, and a shoulder S, cf. text.

tiling and hence to centers of the D tiles of the DHBS tiling. This figure also demonstrates that the atomic structure of larger Pb islands can be understood as a set of starfish clusters. Starfish supported by edge-sharing D tiles share a Pb atom belonging to one of the arms of the starfish. The τP1 tiling thus describes the skeleton of the structure of the ad-

FIG. 8. (Color online) The right part is a section of an experimental 86 Å × 122 Å STM image for 0.2 ML of Pb adsorbed on the five-fold *i*-Al-Pd-Mn surface. A pentagon of the τP1 tiling describes the contrast in STM intensities of the adsorbed Pb island. On the left part its relation to the decagons of the DHBS tiling is shown. In the lower part a direct comparison of calculated STM of the D10T cluster (left) with the experimental image of a starfish is presented. The orientation and the size of the pentagonal protrusions are characterized by the pentagon of the P1 tiling. The rectangle represents the surface of the model derived from the 2/1-approximant.

sorbed Pb islands. Of course, in an extended island atoms will also occupy sites other than those in the starfish clusters. For example, the five D tiles decorating the vertices of a pentagon of the τP1 tiling surround a pentagonal star of the DHBS tiling whose outer vertices are occupied by Pb atoms, but the decoration of the interior of the star tile remains to be determined.
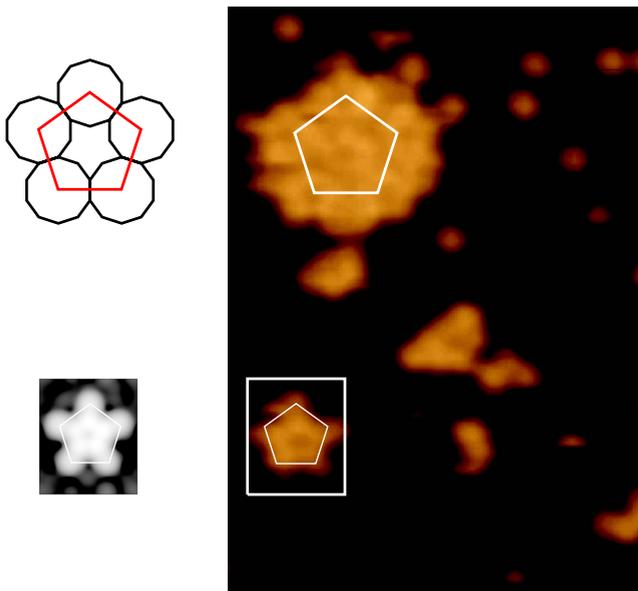
VI. DISCUSSION

The white flower motifs have been identified as preferential nucleation sites first for Si adsorption at low coverage[15] and recently for Bi deposition.[16] In the submonolayer regime, the adsorption of Bi and Pb on the five-fold Al-Pd-Mn surface present some similarities. The diffusion of Bi adatoms leads to the formation of starfish of edge length equal to 4.9 ± 0.2 Å. These pentagonal islands point in the same direction across successive terraces. The dark stars are not preferentially populated upon initial deposition. The number of starfish increases with additional Bi deposition until the system enters a *pure growth regime*.[34] However, this transition takes place around 0.5 ML with the first coalescence of islands whereas it occurs already at 0.2 ML for Pb adsorption [see Fig. 8(b)]. Hence with comparable deposition rates, the mean-free path of diffusing Pb adatoms appears significantly longer than for Bi adsorbates. The mobility of both adsorbates across the terrace is also clearly different. For instance, the "fuzziness" observed on Fig. 2 is not present on STM images reported by Smerdon *et al.*[16] While Bi adatoms are trapped at white flower sites, this is not the case for Pb adsorbates which can depart from these nucleation sites. Thus, we postulate that additional Pb adatoms are necessary to pin the adsorbates at white flower sites and the growth of pentagonal islands. This is consistent with our measurements and calculations which indicate that adatom-adatom interaction plays a crucial role in the stabilization of the Pb starfish. A two-shell structure consisting of ten Pb atoms centered

above the center of the white flower pattern is required to stabilize the starfish motif and its orientation.

Upon further Pb deposition, the density of pentagonal islands increases and additional impinging adatoms fill the interstices of the network. The electronic structure of the complete Pb quasiperiodic monolayer has been probed using scanning tunneling spectroscopy (STS) and ultraviolet photoelectron spectroscopy (UPS).[6] In the experiment, the existence of a deep pseudogap at the Fermi level was demonstrated and the origin of this minimum in the electronic density of states was associated with the quasiperiodicity of the monolayer structure. However alternative explanations can also be considered. For the heavy polyvalent elements photoemission experiments[35–37] show that relativistic spin-orbit coupling leads to a splitting of the $6p$ band into a $p^{1/2}$ and a $p^{3/2}$ component separated by a deep minimum in the electronic density of states. For tetravalent lead this minimum is located precisely at the Fermi level. It exists in the solid (face-centered cubic) phase as well as in the liquid phase, and is confirmed by band-structure calculations.[38,39] To further associate the quasiperiodicity of the Pb film with a deepening of the pseudogap would require fully relativistic electronic structure calculations on our model structure.

VII. CONCLUSION

The initial adsorption of Pb on the five-fold Al-Pd-Mn surface has been investigated using STM along with *ab initio* density-functional calculations. The results show that Pb adatoms are relatively mobile at room temperature and diffuse on terraces to nucleate preferentially above white flower sites. They form pentagonal islands which are described as a two-shell structure consisting of 10 Pb adsorbates. In addi-

tion, the theoretical calculations reveal that this 10-atom starfish is the most stable structure with a binding energy of Pb atoms in the cluster equal to −4.057 eV/Pb atom. The good agreement between the calculated and experimental STM images support the atomic model proposed.

We have demonstrated previously that *ab initio* calculated STM images of the 3/2 approximant model surface reproduce in very fine detail the main features observed experimentally in STM images of the clean five-fold surface of *i*-Al-Pd-Mn.[13] The local atomic arrangement leading to dark star and white flower motifs in STM images were understood, and much insight was gained into the contribution of the different elements to the STM signal. Here, we go a step further and show the validity of using the 2/1 approximant surface as a substrate to model the cluster formed upon heterogeneous adsorption on quasicrystal surfaces. This study emphasizes the importance of using a combined theoretical and experimental approach to the study of complex metallic alloy surfaces.

*Corresponding author.Ledieu@lsg2m.org

†Present address: Department of Chemistry, University of Toronto, Toronto, Ontario M5S 3H6, Canada

[1] B. Unal, C. J. Jenks, and P. A. Thiel, Phys. Rev. B **77**, 195419 (2008).

[2] M. Krajčí and J. Hafner, in *Quasicrystal Surfaces*, edited by Y. Ishii and T. Fujiwara (Elsevier, New York, 2008), p. 313.

[3] K. J. Franke, H. R. Sharma, W. Theis, P. Gille, Ph. Ebert, and K. H. Rieder, Phys. Rev. Lett. **89**, 156104 (2002).

[4] V. Fournée and P. A. Thiel, J. Phys. D **38**, R83 (2005).

[5] H. R. Sharma, M. Shimoda, and A. P. Tsai, Adv. Phys. **56**, 403 (2007).

[6] J. Ledieu, L. Leung, L. H. Wearing, R. McGrath, T. A. Lograsso, D. Wu, and V. Fournée, Phys. Rev. B **77**, 073409 (2008).

[7] M. Krajčí and J. Hafner, Phys. Rev. B **71**, 184207 (2005).

[8] M. Krajčí and J. Hafner, Surf. Sci. **602**, 182 (2008).

[9] T. M. Schaub, D. E. Bürgler, H.-J. Güntherodt, and J.-B. Suck, Phys. Rev. Lett. **73**, 1255 (1994).

[10] J. Ledieu and R. McGrath, J. Phys.: Condens. Matter **15**, S3113 (2003).

[11] Z. Papadopoulos, G. Kasner, J. Ledieu, E. J. Cox, N. V. Richardson, Q. Chen, R. D. Diehl, T. A. Lograsso, A. R. Ross, and R.

McGrath, Phys. Rev. B **66**, 184207 (2002).

[12] G. Kasner and Z. Papadopolos, Philos. Mag. **86**, 813 (2006).

[13] M. Krajčí, J. Hafner, J. Ledieu, and R. McGrath, Phys. Rev. B **73**, 024202 (2006).

[14] T. Cai, J. Ledieu, R. McGrath, V. Fournée, T. A. Lograsso, A. R. Ross, and P. A. Thiel, Surf. Sci. **526**, 115 (2003).

[15] J. Ledieu, P. Unsworth, T. A. Lograsso, A. R. Ross, and R. McGrath, Phys. Rev. B **73**, 012204 (2006).

[16] J. A. Smerdon, J. K. Parle, L. H. Wearing, T. A. Lograsso, A. R. Ross, and R. McGrath, Phys. Rev. B **78**, 075407 (2008).

[17] M. Krajčí and J. Hafner, Phys. Rev. B **71**, 054202 (2005).

[18] M. Krajčí and J. Hafner, Phys. Rev. B **75**, 224205 (2007).

[19] M. Krajčí and J. Hafner, Phys. Rev. B **77**, 134202 (2008).

[20] Single crystals synthesized in the Materials Preparation Center, Ames Laboratory-USDOE, Ames, IA, USA (www.mpc.ameslab.gov).

[21] G. Kresse and J. Furthmüller, Comput. Mater. Sci. **6**, 15 (1996); Phys. Rev. B **54**, 11169 (1996).

[22] G. Kresse and D. Joubert, Phys. Rev. B **59**, 1758 (1999).

[23] J. P. Perdew and Y. Wang, Phys. Rev. B **45**, 13244 (1992).

[24] P. E. Blöchl, Phys. Rev. B **50**, 17953 (1994).

[25] J. Tersoff and D. R. Hamann, Phys. Rev. B **31**, 805 (1985).

[26] M. Cornier-Quiquandon, A. Quivy, S. Lefebvre, E. Elkaim, G. Heger, A. Katz, and D. Gratias, Phys. Rev. B **44**, 2071 (1991).

[27] A. Katz and D. Gratias, J. Non-Cryst. Solids **153-154**, 187 (1993).

[28] M. Boudard, M. de Boissieu, C. Janot, G. Heger, C. Beeli, H.-U. Nissen, H. Vincent, R. Ibberson, M. Audier, and J. M. Dubois, J. Phys.: Condens. Matter **4**, 10149 (1992).

[29] M. de Boissieu, P. Stephens, M. Boudard, C. Janot, D. L. Chapman, and M. Audier, J. Phys.: Condens. Matter **6**, 10725 (1994).

[30] M. Krajčí, M. Windisch, J. Hafner, G. Kresse, and M. Mihalkovič, Phys. Rev. B **51**, 17355 (1995).

[31] C. Ghosh, Da-Jiang Liu, K. J. Schnitzenbaumer, C. J. Jenks, P. A. Thiel, and J. W. Evans, Surf. Sci. **600**, 2220 (2006).

[32] Z. Papadopolos, P. Pleasants, G. Kasner, V. Fournée, C. J. Jenks, J. Ledieu, and R. McGrath, Phys. Rev. B **69**, 224201 (2004).

[33] D. Gratias, F. Puyraimond, M. Quiquandon, and A. Katz, Phys. Rev. B **63**, 024202 (2000).

[34] H. Brune, Surf. Sci. Rep. **31**, 121 (1998).

[35] F. R. McFeely, L. Ley, S. P. Kowalczyk, and D. A. Shirley, Solid State Commun. **17**, 1415 (1975).

[36] G. Indlekofer, P. Oelhafen, R. Lapka, and H. J. Güntherodt, Z. Phys. Chem., Neue Folge **157**, 465 (1988).

[37] J. T. M. Wotherspoon, D. C. Rodway, and C. Norris, Philos. Mag. B **40**, 51 (1979).

[38] N. E. Christensen, S. Satpathy, and Z. Pawlowska, Phys. Rev. B **34**, 5977 (1986).

[39] W. Jank and J. Hafner, Phys. Rev. B **41**, 1497 (1990).